# Electrophysical properties of metal–solid-electrolyte composites

S. Gluzman
*Institut für Energieverfahrenstechnik, Forschungszentrum Jülich GmbH (KFA), D-52425 Jülich, Germany*

A. A. Kornyshev
*Institut für Energieverfahrenstechnik, Forschungszentrum Jülich GmbH (KFA), D-52425 Jülich, Germany* and The A. N. Frumkin Institute of Electrochemistry of the Academy of Sciences, 117071 Moscow, Russia*

A. V. Neimark
*Institut für Anorganishe and Analytishe Chemie, Iohannes-Gutenberg Universität Mainz, D-55099 Germany and Laboratorie Phenomenes de Transport dans les Melanges, C.N.R.S., F-86360 Chassenenil du Poitou, France*
(Received 31 May 1994; revised manuscript received 20 December 1994)

An effective-medium theory of a random mixture of metal and solid electrolyte particles is developed to describe the bulk ac conductance of the composite. It predicts a 4 to 6 orders of magnitude enhancement of the dielectric permeability of the composite near the percolation threshold for electronic conductivity. As the frequency increases, the enhancement falls to the level of a metal-dielectric composite, as the role of the double-layer capacitance of the blocking interfaces between metal and electrolyte grains diminishes. Analytical expressions are obtained for the conductivity and dielectric function over the whole range of relative concentrations and in a broad frequency range.

## I. INTRODUCTION

### A. Metal-solid electrolyte composites

There is presently great interest in dual-phase composites of electronic and fast ionic conductors. These are, in particular, membranes with solid electrolyte components in which oxygen anions or protons are the conducting species used for separations and heterogeneous chemical reactions.[1] In such systems the metal component plays the role of an electronically conductive catalyst or supporter that provides a smooth contact of the membrane with the bulk metal electrodes.[2] Typical examples are ceramic mixtures of yttria-stabilized zirconia (YSZ) and nickel or palladium granules, the systems regarded as promising materials for hydrogen electrodes in solid oxide fuel cells.[1] On the other hand, systems of this kind could be of interest as materials with unusual dielectric properties.

The electrophysical properties of composite materials are frequently described in terms of percolation theory.[3–5] Single- and dual-component systems have been considered, including clusters of conducting granules and mixtures of a conductor and superconductor, an ionic conductor and insulator, and metal and insulator particles.[6–16] A mixture of conductors of the first and second kind, such as a metal–solid-electrolyte composite, contains some features which other composites do not possess, which makes these composites interesting from the fundamental point of view, as well. These features are as follows.

(i) Solid electrolyte granules are ionic conductors, the conductivity being, usually, a few orders of magnitude smaller than the electronic conductivity of the metal.

(ii) There is no dc current across the interface of the electronic conductor and ionic conductor, unless some Faraday process (electrochemical reaction) takes place at the interface.

(iii) An electric double layer of microscopic dimensions is formed at the blocking metal/solid-electrolyte contact with the double-layer capacitance $\gtrsim 10\ \mu\mathrm{F/cm^2}$, a value some $10^3-10^5$ times greater than the geometrical capacitance of insulator particles of the same size (in the range of micrometers and greater).

(iv) While the metal/solid-electrolyte contact is blocking for dc, it can conduct ac current in the same way as a metal/dielectric interface, but the characteristic frequencies for the former are much lower. These frequencies are determined by the relaxation time needed to charge the double layer via the migration of ions through the bulk of the electrolyte to the interface.[17] This time is $\sim l_d l/D$, where $D$ is the diffusion coefficient of mobile ions, $l_d$ is the Debye length in the solid electrolyte, while $l$ is the thickness of the solid electrolyte particles.[17] In composites, the size of the grain will stand for $l$, i.e., the relaxation time will be proportional to the size of the grain. For a particle of 1 $\mu$m size the typical relaxation time $\sim 10^{-5}-10^{-6}$ s. The relaxation should give rise to a pronounced frequency dispersion of dielectric permittivity in the MHz range, at frequencies the lower the larger the granules.

### B. Metal/composite/metal structures

There is, however, a principal difference between metal-insulator and metal–solid-electrolyte mixtures due to electric double-layer formation at the metal/solid-electrolyte interface. The latter does not let a static electric field penetrate into the bulk of the composite below the percolation threshold in the metal component.

 

Above the threshold there is a potential drop across the sample, as far as the electronic current passes through it.

Placing the sample between two blocking (for ionic current) electrodes creates a metal/composite/metal (MCM) structure. There are several regimes of the MCM electric response.

For a composite below the percolation threshold, at zero frequency, the MCM structure works as a double-layer capacitor. On each electrode, the connected clusters of metal grains of the composite, touching the surface of the metal plate, effectively extend the electrode surface into the bulk. Indeed, the metal plates contact the electrolyte directly or via the metal clusters of the composite connected to the plates forming the effective electrode surface (see Fig. 1). The closer we are to the percolation threshold, the larger is the surface of such an "electrode," but below the threshold there is still no short cut between the two opposing electrodes in a sufficiently thick sample. The idea of enhancing by orders of magnitude the effective electrode/electrolyte interface by making a contact of a flat metal plate with the metal-containing composite was widely used in a number of technical designs, including supercapacitors. In order to avoid the eventual short cut in a supercapacitor a separating layer free from metal components (i.e., a membrane, made of the same electrolyte) is disposed between two such electrodes.[18] The static electric field is fully screened at the double-layer distances (which are much smaller than the grain size) near the effective electrode surfaces. Since the interfaces between the metal plates and the electrolyte and between the metal clusters and electrolyte are blocking, there is no dc current in this case across the MCM structure, i.e., it is blocking as a whole and can be used as a capacitor.

However, an ac signal penetrates into the sample bulk at frequencies greater than the inverse time needed to charge the double layers near the effective electrode surface. This time is determined by the migration transport of the mobile ions through the bulk of the solid electrolyte from one effective surface to another. The migration time is evaluated as $LL_d/D$, where $L$ is the thickness of the sample including the membrane if there is one, $L_d$ is the thickness of the double layer (in simple models it coincides with the Debye length in the electrolyte). At shorter times the double layer is not yet set up at the interface to screen the field. An ac current with frequencies greater than $D/LL_d$ then passes across the MCM structure as the ac field penetrates into the bulk of the composite. Both metal and solid electrolyte conductances will contribute to the ac conductivity of the system; one may also speak in this case about the frequency dependent dielectric properties of the bulk.

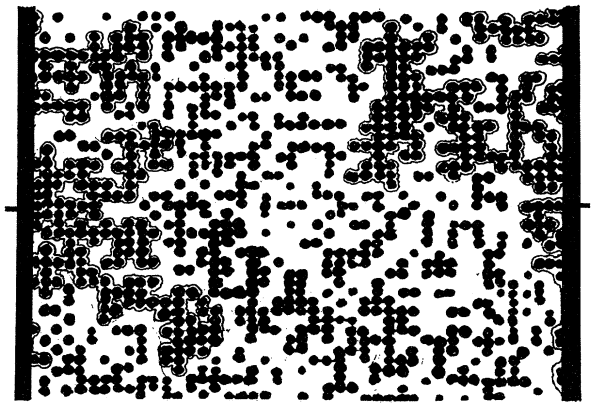

FIG. 1. A schematic picture of a cross section of the metal/composite/metal (MCM) system. Black spots denote metal particles; white space in between is filled by the particles of solid electrolyte. The lines show the surface of the clusters connected with the metal electrodes, i.e., they determine the "effective electrode surface." The picture is based on two-dimensional random site percolation on a square grid at $x=0.5$ [$x_c=0.593$ (Ref. 5)]; the cross section of three-dimensional percolation on a cubic lattice will look different.

### C. Bulk and surface contributions: MCM admittance

When the composite is below the percolation threshold in the metallic component, the response of the MCM system may be represented by an approximate equivalent circuit (Fig. 2). Here the blocking capacitance $C_d$ is the capacitance of the double layer at the effective metal/solid-electrolyte interface,

$$C_d=\frac{\epsilon_0 S_{\text{eff}}}{4\pi L_d}\ , \tag{1}$$

where $S_{\text{eff}}$ is the effective surface area and $\epsilon_0$ is the dielectric constant of the ionic crystal at frozen mobility of the ions (the high-frequency dielectric constant). $C_g$ is the geometric capacitance of the sample,

$$C_g=\frac{\epsilon S}{4\pi L}\ , \tag{2}$$

where $S$ is the surface area of the plates and $\epsilon$ is the bulk dielectric constant of the composite. $R_g$ is the geometric resistivity of the composite.

This circuit should be valid for a sample that is much thicker than the size of the largest percolation cluster and only in an "interpolation sense," because it gives proper results at $\omega=0$ and $D/LL_d \ll \omega \ll D/lL_d$, but one cannot guarantee that it would work at intermediate frequencies $0 \ll \omega \ll D/LL_d$. It is well known that roughness of

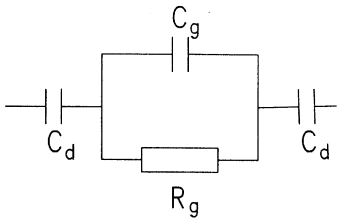


FIG. 2. An approximate equivalent circuit of metal/composite/metal systems below percolation in the metallic component. $C_d$ is the interfacial double-layer capacitance and $C_g$ and $R_g$ are the geometrical capacitance and resistance of the composite.

the electrode surface gives rise to the so called constant phase element (CPE) behavior: $Y \propto (-i\omega)^p$ with $p < 1$. After a provocative suggestions of Le Mehaute and Crepy[19] that the exponent $p$ is determined by the Hausdorff dimension of the interface, $D_i$, a number of papers were published on the study of the CPE impedance for model fractal surfaces of blocking electrodes.[19,20] Inspired by the pioneering paper of De Levi,[21] who has treated a deep pore as an ac transmission line, these works have considered hierarchical pore models of the interface which could be described as self-affine fractals. It was shown for model self-affine structures, both theoretically and experimentally, that there is no universal relationship between $p$ and $D_i$.

However, the effective metal/electrolyte interface, which emerges in the MCM structure close to the percolation threshold in the metallic component, in the case of particles of equal size is rather self-similar than self-affine. As shown recently by Halsey and Leibig,[22] the surfaces of self-similar objects do contribute to the CPE behavior (as an intermediate asymptotic of the impedance, limited by the frequencies from below and above; they obtained explicit expressions for the cross-over frequencies), but under a certain condition: if the correlation dimension of the harmonic measure of the surface $\tau(2)$ (the probability measure defined by the normal component of electric field at the surface[23]) is not equal to $D_i$. A difference between the values of the two exponents is a manifestation of a multifractal structure of the surface. We are not aware of calculations of $\tau(2)$ for the surfaces of percolation clusters. *A priori,* the reasons why these structures should exhibit multifractal properties are not obvious, and this question requires a special study. In real systems there could be many reasons which would make the interfaces multifractal. Keeping in mind our idealized percolation model we would, however, neglect at first instance any CPE contribution.

Hereafter, the complex admittance is defined as a current response to the voltage signal $\sim\exp(-i\omega t)$ (which determines the negative sign of the capacitance contribution). The equivalent circuit shown in Fig. 2 has three frequency independent elements. However, for the purposes of our discussion, the admittance can be formally rewritten in terms of two frequency dependent parallel-connected effective elements, the effective conductance and effective capacitance:

$$Y(\omega)=\sigma_{\text{eff}}(\omega)-i\omega C_{\text{eff}}(\omega) , \tag{3}$$

where

$$\sigma_{\text{eff}}(\omega)=\frac{1}{R_g}\left[1-\frac{\omega_1}{\omega_2}\right]\frac{\omega^2}{\omega_1^2(1+\omega^2/\omega_1^2)} , \tag{4}$$

$$C_{\text{eff}}(\omega)=C_d/2\frac{1+\omega^2/\omega_1\omega_2}{1+\omega^2/\omega_1^2} , \tag{5}$$

and

$$\omega_1=\frac{2}{C_dR_g},\quad \omega_2=\frac{1}{C_gR_g} . \tag{6}$$

$C_d > C_g$ and in most cases $C_d \gg C_g$, so that $\omega_2 \gg \omega_1$. At $\omega \ll \omega_1$, $\sigma_{\text{eff}}(\omega)\approx 0$ and $C_{\text{eff}}(\omega)\approx C_d/2$ (the limit of interface blocking). At $\omega \gg \omega_1$, $\sigma_{\text{eff}}(\omega)\approx R_g^{-1}$, and at $\omega \gg \sqrt{\omega_1\omega_2}$, $C_{\text{eff}}(\omega)\approx C_g$.

A simple evaluation of $S_{\text{eff}}$ can be given in a fractal regime,

$$S=RL^2 , \tag{7}$$

where the roughness factor

$$R=(L/l)^{D_p-2}(l/r_0)^{D_s-2} . \tag{8}$$

Here $r_0$ is the smallest self-similarity range on the surface of one metal granule, and $D_p$ and $D_s$ are, respectively, the fractal dimensions of the surface of the percolation cluster and of the interface between the two grains (metal/electrolyte). $D_p > 2$, while $D_s$ can be greater or smaller than 2 depending on whether the contact between the grains is good or bad. The upper physical limit for the roughness factor is obtained by putting $D_p = D_s = 3$, which gives $R \propto L/r_0 (\propto 10^7$ for a sample with 1 cm$^2$ cross section, but typical estimates would give $R < 10^4$). Together with Eq. (1) this gives an estimate for $C_d$, exact calculation of which is a complicated task.

### D. The goal and the structure of the paper

The main subject of our work will be the calculation of $R_g$ and $C_g$, i.e., of the bulk characteristics of the sample. However, comparing the theory with experiments, we will focus on the interplay between the bulk and surface contributions.

Close to the percolation threshold, where an infinite passage through the metal granules emerges, one may expect a strong enhancement of the imaginary part of the system conductance, i.e., the anomalously large dielectric permittivity. A similar effect, known as the "dielectric catastrophe" has been obtained theoretically[8,10] and experimentally observed in metal-dielectric composites.[13] However, in the metal/solid-electrolyte composites the effect could be, actually, much larger because the capacitance of the double layer at the contact of the metal and solid electrolyte grains is a few orders of magnitude greater than the geometrical capacitance of dielectric grains of the same size.

With these expectations in mind one may try to build a percolation-type theory of the bulk conductance of metal/solid-electrolyte composites. As a first attempt, it is expedient to start with an extension of the effective-medium theory proposed by Kirkpatrick[6] for dc conductivity, which gives in our case a simple analytical solution, formally in the whole range of the relative composition and a broad range of frequencies. Such a theory is developed in the present paper.

In the next section we formulate the model of the composite as a three-bond random network and adopt the equivalent circuits for the bonds. In Sec. III we discuss the basic parameters of the model and estimate their values. In Sec. IV we develop two variants of the effective-medium formalism for the random metal–solid-electrolyte mixture. Results for the real and imaginary

parts of the conductance are discussed in Sec. V. Simple approximate analytical formulas are derived in Sec. VI, using the smallness of some parameters typical for experiments with real composites. Order of magnitude estimates and the dependence of the predicted effects on temperature and other factors are given in Sec. VII. In Sec. VIII we discuss the proper way of comparison with experimental data, together with some previous theoretical studies.

## II. THE MODEL OF A RANDOM METAL/SOLID-ELECTROLYTE MIXTURE

We start with a square (cubic) lattice with a fraction $x$ of randomly chosen occupied squares (cubes), which represent the metallic material (black) (see Fig. 3). Correspondingly, the fraction of the solid electrolyte component (white) is $1-x$. The links between centers (sites) of the nearest neighbor squares (cubes) are called bonds. Bonds between two black sites have an admittance $\Sigma_1(\omega)$ with $\Sigma_1(0)\neq 0$, which characterizes the metallic component. Bonds between two white sites have an admittance $\Sigma_2(\omega)$ with $\Sigma_2(0)\neq 0$ $[\Sigma_2(0)\ll\Sigma_1(0)]$, which characterizes the solid electrolyte. Bonds between black and white sites have an admittance $\Sigma_3(\omega)$ with $\Sigma_3(0)=0$, which represents the blocking metal/solid-electrolyte interface.

We adopt the following expressions for the bond conductances:[17]

$$\Sigma_1 \equiv \sigma_1 , \tag{9}$$

$$\Sigma_2(\omega)=\sigma_2 - iC_2\omega . \tag{10}$$

Here $\sigma_1$ and $\sigma_2$ differ from the bulk conductivity of the metal and solid electrolyte, respectively, by a factor related to the size of the granule. (For grains of the same size $\sigma_1/\sigma_2$ is equal to the ratio of the corresponding bulk conductivities.) $C_2$ is the geometrical capacitance of the solid electrolyte cube, i.e., the capacitance of the solid electrolyte grain when the ions are frozen. $\Sigma_3(\omega)$ corresponds to the equivalent circuit of Fig. 4:

$$\Sigma_3(\omega)=-iC_3\omega\left[1-\frac{iC_3\omega}{2\sigma_1}-\frac{iC_3\omega}{2\Sigma_2(\omega)}\right]^{-1} , \tag{11}$$

where $C_3$ stands for the capacity of the metal/solid-electrolyte interface. This is the simplest model for the blocking metal/solid-electrolyte contact; it behaves as a double-layer interfacial capacitance at zero frequency, but it conducts the relaxation current. At frequencies higher than the inverse time needed to charge the double layer through the bulk of the solid electrolyte, the interfacial element does not influence the ac current.

Note that in Eq. (9) the frequency dispersion of the metal conductivity, which is frequently described by the Drude formula, is ignored because we are interested in the range of much lower frequencies, not exceeding considerably the characteristic frequency of charging the double layer by ion migration through the grains ($\omega \lesssim 10^7$ $s^{-1}$, see Sec. III). For the same reason we neglected the infrared frequency dispersion of $C_2$, since these frequencies are also far beyond the frequency range that we focus on. More severe assumptions are made on the equivalent circuit that results in Eq. (11). There could be a number of elementary processes not accounted for by this circuit, which can give rise to a dispersion at low frequencies.[24] For instance, it does not involve Faraday processes across the interface, which will contribute a shunt: a "reaction" resistance parallel to $C_3$, so that the contact will be no longer blocking. Possible roughness of the interface between the metal and solid electrolyte grains leads to a constant phase element.[20] Wartburg impedance due to diffusion of minority carriers can contribute as well.[24] More complicated variants of the equivalent circuit for the third bond will be discussed elsewhere. In the present paper we wish to get the "reference" results for the most simple, basic equivalent circuit with the three elements always present in any metal/solid-electrolyte system.

The fractions of electron conducting, ion conducting, and "blocking" bonds are given, respectively, by the expressions

$$p_1=x^2,\quad p_2=(1-x)^2,\quad p_3=2x(1-x) , \tag{12}$$

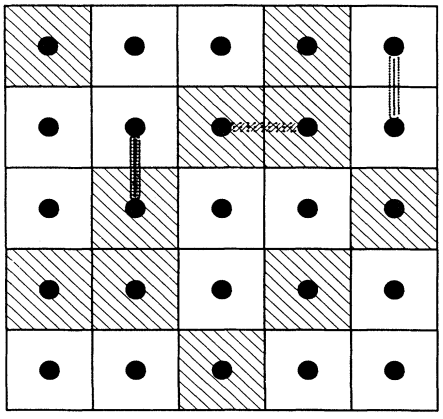

FIG. 3. Two-dimensional picture of the percolation system. Black and white squares correspond to metal and solid electrolyte particles, respectively. Centers of the squares correspond to lattice sites. Bonds between two black sites, two white sites, and black and white sites are shown by wavy, thin, and solid lines, respectively. In the three-dimensional case squares should be substituted by cubes.

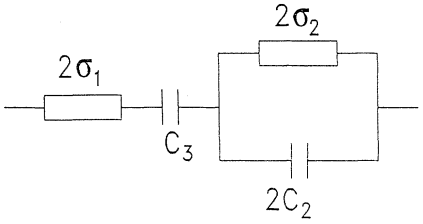


FIG. 4. Equivalent circuit of the third bond. $\sigma_1$ and $\sigma_2$ are the conductivities of metal and solid electrolyte grains, respectively, $C_2$ the geometrical capacitance of the solid electrolyte grains, $C_3$ the capacitance of the interface between the metal and solid electrolyte grains.

which are prescribed by the random site distribution. Then the value of a complex bond conductance $\sigma$ is distributed according to a probability density $f(\sigma)$

$$f(\sigma)=p_1\delta(\sigma-\Sigma_1(\omega))+p_2\delta(\sigma-\Sigma_2(\omega)) +p_3\delta(\sigma-\Sigma_3(\omega)) . \quad (13)$$

Our task, now, is to solve the corresponding system of the Kirchhoff equations on the cubic lattice with three types of conductances (bonds) distributed according to the distribution function (13).

More complicated distribution functions can be proposed in order to take into account some real features of the composite. For example, a nonuniformity of its phase state, caused by preparation conditions, will lead to a random distribution of bond conductances over some finite intervals of allowed values. The presence of spherical voids with random positions can be considered as well, resulting in power-law type distribution functions.[4] In this paper, however, we limit the analysis to the simplest case, described by Eq. (13).

## III. SYSTEM PARAMETERS

We scale the system parameters to the unit values of the conductivity of the metal and the geometric capacitance of the solid electrolyte and set the lattice spacing equal to unity, so that bond conductances and conductivities have the same dimension. In these units $\sigma_1=1$ and $C_2=1$ and the typical orders of magnitude of the other two parameters correspond to $\sigma_2=10^{-3}$ and $C_3=10^3$. There are superionic conductors for which $\sigma_2$ reaches 1 (in the units of conductivity of the poorest electronic conductors), but for most metal-electrolyte combinations the ratio is orders of magnitude lower.

The system characteristic frequencies are

$$\omega_{2,2}=\frac{\sigma_2}{C_2},\quad \omega_{1,3}=\frac{2\sigma_1}{C_3},\quad \omega_{2,3}=\frac{2\sigma_2}{C_3} . \quad (14)$$

$\omega_{2,2}^{-1}$ is the characteristic time of charging the capacitor with the geometric capacitance of the solid electrolyte grains. $\omega_{1,3}^{-1}$ and $\omega_{2,3}^{-1}$ are the times of charging the double layer at the metal/solid-electrolyte interface by electron transport through the bulk of the metal and by migration of ions through the bulk of the solid electrolyte, respectively. The migration frequency $\omega_{2,3}$ is the lowest and most important of the fundamental frequencies when one works in the range of relatively low $\omega$. In the dimensionless units given above the corresponding frequency estimates are

$$\omega_{2,2}\sim 10^{-3},\quad \omega_{1,3}\sim 2\times 10^{-3},\quad \omega_{2,3}\sim 10^{-6} . \quad (15)$$

These estimates are supported by the following considerations. The capacity of the metal/solid-electrolyte contact $C_3=C_D l^2$, where $C_D$ is the double layer capacity per unit surface area and $l^2$ the contact area between the metal and solid electrolyte grains ($l^2\lesssim$ the mean cross section of the grain). $C_D$ can be roughly evaluated as $\simeq\epsilon_*/4\pi l_d$, where $l_d$ is the Debye length ($\sim 1-10$ Å) and $\epsilon_*$ is the dielectric constant of the immobile skeleton of the solid electrolyte ($\sim 5-10$). The geometrical capacitance $C_2\simeq\epsilon_* l^2/4\pi l=\epsilon_* l/4\pi$. Then

$$\omega_{2,2}\simeq\frac{4\pi\sigma_2}{\epsilon_*} , \quad (16)$$

$$\omega_{2,3}\simeq\frac{4\pi\sigma_2 l_d}{\epsilon_* l} , \quad (17)$$

$$\omega_{1,3}\simeq\frac{4\pi\sigma_1 l_d}{\epsilon_* l} . \quad (18)$$

Let us take for estimates

$$\sigma_1=0.5\times 10^5\ \Omega^{-1}\,\mathrm{cm}^{-1},\quad \sigma_2=5\times 10^{-1}\ \Omega^{-1}\,\mathrm{cm}^{-1} ,$$

$$\frac{l_d}{l}=10^{-4},\quad \epsilon_*=5 .$$

Then

$$\omega_{2,2}=10^{11}\ \mathrm{s}^{-1},\quad \omega_{2,3}=10^7\ \mathrm{s}^{-1},\quad \omega_{1,3}=10^{12}\ \mathrm{s}^{-1} .$$

In general the conductivity of metals and solid electrolytes lies within the ranges $10<\sigma_1<10^5\ \Omega^{-1}\,\mathrm{cm}^{-1}$ and $10^{-3}<\sigma_2<10\ \Omega^{-1}\,\mathrm{cm}^{-1}$, respectively. Depending on the size of the grains $10^{-5}<l_d/l<10^{-3}$. This defines the ranges for the characteristic frequencies $10^8<\omega_{2,2}\lesssim 10^{12}\ \mathrm{s}^{-1}$, $10^3<\omega_{2,3}<10^{10}\ \mathrm{s}^{-1}$, and $10^7<\omega_{1,3}<2\times 10^{13}\ \mathrm{s}^{-1}$. In the case of very high superionic conductivity of the electrolyte and very low electronic conductivity of the metal these frequency regions can overlap. However, this is an extreme situation and for most realistic metal/solid-electrolyte mixtures the frequencies are well separated. The frequency $\omega_{2,3}$ is the lowest one and the only frequency of interest in the electrical impedance measurements, where one cannot go higher than $10^7\ \mathrm{s}^{-1}$.

## IV. EFFECTIVE-MEDIUM THEORY

The conductance of the system can be expressed through the conductivity $\sigma$ and typical linear size $L$ of the system as $\sigma L^{d-2}$, where $d$ is the dimensionality of the system. Our task is then to calculated some intensive characteristics of the composite material as the complex conductivity $\sigma(\omega)$ and the dielectric permittivity. The latter is related to $\sigma(\omega)$ by the equation $\epsilon(\omega)=1+4\pi i\sigma(\omega)/\omega$; the dielectric susceptibility is defined as $\chi(\omega)=[\epsilon(\omega)-1]/4\pi$. We will study below the quantities

$$\sigma'=\mathrm{Re}\sigma(\omega) \quad (19)$$

and

$$\chi'=\mathrm{Re}\chi(\omega)=-\frac{\mathrm{Im}\sigma(\omega)}{\omega} . \quad (20)$$

The random network will be treated by means of two variants of effective-medium theory, which allows us to obtain approximate solutions of the Kirchhoff equations in the quasistationary limit (see Sec. I).

### A. Single-bond approximation

In the so-called single-bond (SB) effective-medium approximation the conductivity $\sigma$ obeys the equation[6]

$$\int f(\tilde{\sigma})d\tilde{\sigma}\frac{\sigma-\tilde{\sigma}}{\tilde{\sigma}+(d-1)\sigma}=0 .$$

Substituting into this equation the distribution function (13) one obtains an equation on $\sigma$:

$$p_1\frac{\sigma-\Sigma_1}{\Sigma_1+(d-1)\sigma}+p_2\frac{\sigma-\Sigma_2}{\Sigma_2+(d-1)\sigma}+p_3\frac{\sigma-\Sigma_3}{\Sigma_3+(d-1)\sigma}=0 . \quad (21)$$

This would allow us to obtain expressions for $\sigma'$ and $\chi'$.

There are limiting cases of this equation which have been studied before. When $\Sigma_3(\omega)$ is put equal to $\Sigma_2(\omega)$ [Eq. (10)], Eq. (21) reduces to the one used for a description of the two-component mixture of metal–"leaky" dielectric particles.[3] The limit $\Sigma_2(0)=0$ has been considered for the two-component mixture of metal-insulator particles.[3]

This model works satisfactorily for bond disordered systems, but is known to give inaccurate results, primarily for the positions of the percolation thresholds, for the site disordered system on which our problem was mapped.[11] The SB approximation neglects completely correlations between the values of the conductivity of bonds with a common site. Nevertheless, we use this model as a "zero" approximation since it leads to relatively simple analytical results and in order to see the effect of correlations by comparing the SB model with more refined models.

### B. Low-concentration cluster approximation

As a next approximation, treating clusters larger than one bond we employ the so called "low-concentration cluster" (LC) effective-medium theory suggested by Bernasconi and Wiesmann,[11] which is an analog of the Bethe approximation in the Ising model. This approximation considers explicitly the cluster of bonds which have a common site, all the other bonds being treated as an effective medium; thereby it takes into account at least part of the correlation between the values of bonds with a common site. This model is expected to give better values of percolation thresholds than the SB model. It leads to the following equation on conductance $\sigma$:[11]

$$p_1\frac{1}{\Sigma_1+q\sigma}+p_2\frac{1}{\Sigma_2+q\sigma}+p_3\frac{1}{\Sigma_3+q\sigma}-\frac{1}{(1+q)\sigma}=0 , \quad (22)$$

where $q=2/(\pi-2)=1.752$ at $d=2$ and $q=3.7655$ at $d=3$. For $d=2$ the Bernasconi-Wiesmann model is equivalent to the Watson-Leath model.[7]

Since $p_1+p_2+p_3=1$, simple algebra shows that Eq. (22) is identical to Eq. (21), if one replaces $(d-1)$ by $q$, and that the resulting equation is cubic on $\sigma$:

$$p_1\frac{\Sigma_1}{\Sigma_1+q\sigma}+p_2\frac{\Sigma_2}{\Sigma_2+q\sigma}+p_3\frac{\Sigma_3}{\Sigma_3+q\sigma}=\frac{1}{(1+q)} .$$

It will be used together with Eqs. (9)–(11) to find the real and imaginary parts of the complex conductivity where only the root which provides $\mathrm{Re}\sigma>0$ will be kept in the studied range of frequencies. This condition is not satisfied for the two conjugated roots, but could be fulfilled for the lone root. In the "quasi"-dc case ($\omega$ is smaller than all the frequencies of the model except $\omega_1$) the equation on $\sigma$ degenerates into quadratic equations, while in the general case one has to use a cumbersome Cardano formula.

In the next two sections we consider results for conductivity and permittivity in three dimensions (3D).

## V. RESULTS FOR THREE-DIMENSIONAL CASE

### A. Real part of conductance

The overall conductivity, measured in a gedanken setup which does not distinguish the sort of charge carriers, is composed of ionic and electronic contributions. This quantity is shown in Fig. 5, where the plot of $\ln(\sigma'/\sigma_2)$ reveals the behavior in the region $x \lesssim x_c$ dominated by the ionic conductivity. It thus displays a quasithreshold behavior manifested in a sharp rise of conductivity above $x_c$. However, in real steady state measurements of Ohmic resistance with electronically conductive leads, the solid electrolyte contribution to the current will be absent and the true metal-conductance threshold will be observed. At the same time both contributions will be seen at high frequencies, when the metal/electrolyte contact is no longer blocking.

The threshold values for electronic conductivity follow from Eq. (21) or Eq. (22) by putting there formally $\Sigma_2=\Sigma_3=0$: in 3D this gives $x_c=0.577$ (for the SB approximation) or $=0.458$ (for the approximation LC). Both values of the threshold are higher than the best known value for the one-component random site problem $x_c=0.3116$.[3] Note that the LC approximation gives a better value. The quasithreshold value practically coincides with the thresholds.

The ac conductivity of the SB model at three different frequencies is displayed in Fig. 6(a); for the LC model

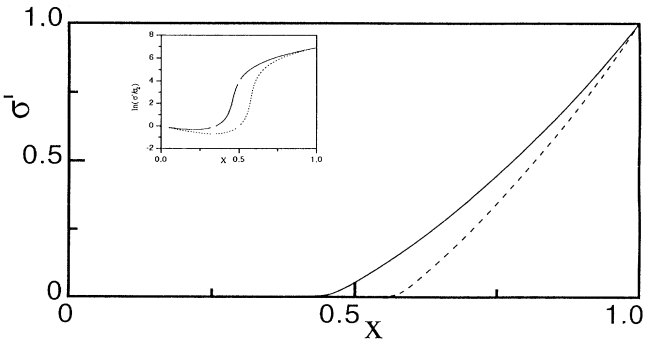


FIG. 5. Low-frequency conductivity (in units of the bulk conductivity of the metallic component) of LC (solid line) and SB (dotted line) models in 3D as a function of fraction $x$. The logarithmic plot, shown as an inset, shows the nonzero conductivity below the percolation threshold in the metallic component due to the conductivity of the solid electrolyte component, $\sigma_2$. (Parameters: $\sigma_1=1$, $\sigma_2=10^{-3}$.)

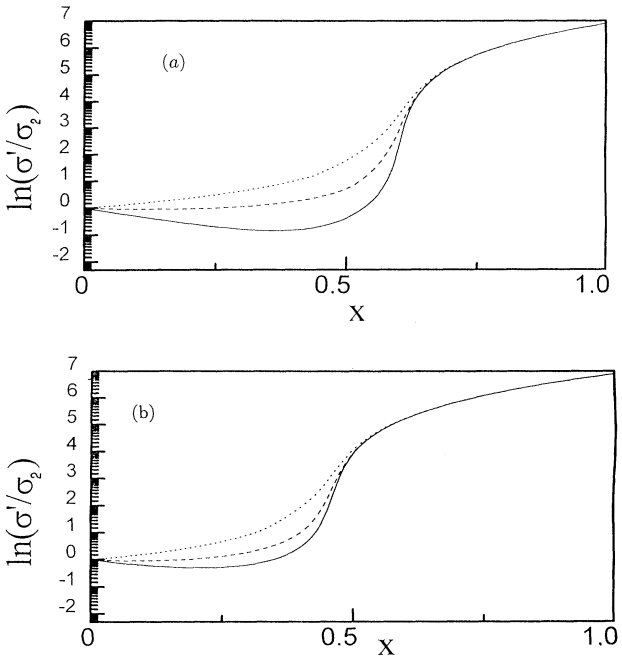


FIG. 6. The ac conductivity (in units of the bulk conductivity of the metallic component) in 3D as a function of $x$ at three different frequencies. Solid lines correspond to low frequency ($\omega=10^{-10}$), dashed line, to intermediate ($\omega=10^{-6}$), and dotted lines to high frequency ($\omega=10^{-3}$). (a) SB model and (b) LC model. Frequencies are given in units of $\omega_{2,2}/\gamma$ (for typical estimates $\omega_{2,2}/\gamma\sim10^{12}$ $s^{-1}$). (Parameters: $\sigma_1=1$, $C_2=1$, $\sigma_2=10^{-3}$, $C_3=10^3$.)

analogous curves are shown in Fig. 6(b). We see that the conductivity rises with increasing frequency, because the higher the frequency the greater is the conductance of the third bond (the double-layer capacitance becoming less and less important).

### B. Dielectric susceptibility

The results for the effective dielectric susceptibility $\chi'$ as a function of $x$ for fixed $\omega$ (Fig. 7) are qualitatively similar for both models. The peaks are centered at $x_c=0.577$ (SB model) and $x_c=0.458$ (LC model).

The frequency dependence of $\chi'$ for two values of $x$ is shown in Figs. 8(a) and 8(b). It has a typical Lorentzian form

$$\chi'(\omega)\sim\frac{1}{1+(\omega/\omega_{2,3})^2}\ . \tag{23}$$

[The plot of $(\chi')^{-1}$ versus $\omega^2$ gives, indeed, a straight line with a slope equal to $\omega_{2,3}^{-2}$.]

The value of the dielectric susceptibility at the percolation threshold through the metallic component can be evaluated as

$$\chi'(0,x_c)\sim C_3\left[\frac{\sigma_1}{\sigma_2}\right]^{1/2}\ . \tag{24}$$

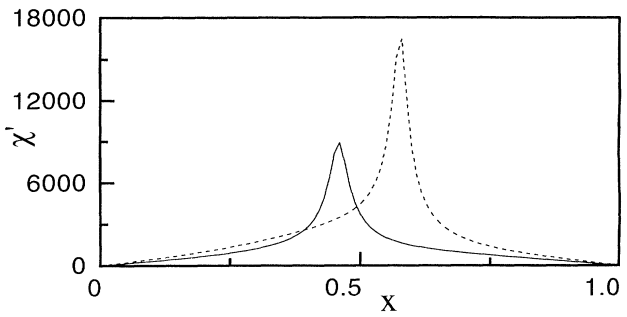


FIG. 7. The results for the real part of the susceptibility $\chi'$ in 3D as a function of $x$ for $\sqrt{\omega_1\omega_2}<\omega\ll\omega_{2,3}$; dotted line, SB model and solid line, LC model. (Parameters: $\sigma_1=1$, $C_2=1$, $\sigma_2=10^{-3}$, $C_3=10^3$.)

We expect that for a real 3D system the critical exponent will take a value different from 0.5.

At $\omega\gg\omega_{2,3}$ the system behaves effectively as a metal–solid-electrolyte mixture, but with a minor contribution of the interface between the metal and solid electrolyte grains. The dielectric susceptibility of the system at low frequencies is greater by a factor of $C_3/C_2$. In order to clarify this point we present in Fig. 9 the results given by the three-bond theory within the framework of the LC model and the "2-bond theory," which ignores the effects of the interface, which is formally a particular case of the three-bond model: $\Sigma_3\equiv\Sigma_2(\omega)$. With increasing frequency, the difference between the three-bond and two-bond theories almost disappears.[25]

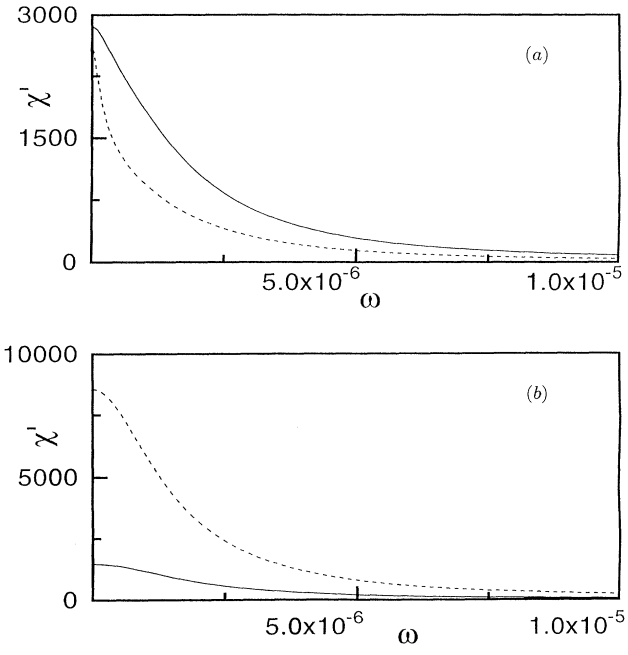


FIG. 8. The frequency dependence of $\chi'$ in 3D, $x=0.4$ and $x=0.6$; solid line, LC model; dotted line, SB model. (Parameters: $\sigma_1=1$, $C_2=1$, $\sigma_2=10^{-3}$, $C_3=10^3$.)

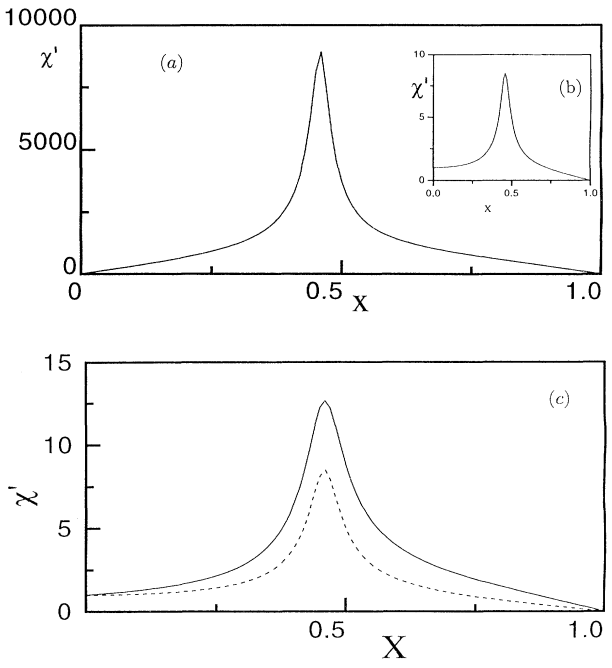


FIG. 9. The real part of the susceptibility as a function of $x$, LC model, formal limit of $\omega=0$: (a) three-bond description; (b) two-bond limit (see discussion in the text); (c) the results of three-bond (solid line) and two-bond (dashed line) models are compared at high frequency $\omega=10^{-4}$. Frequency units the same as in Fig. 6. (Parameters: $\sigma_1=1$, $C_2=1$, $\sigma_2=10^{-3}$, $C_3=10^3$.)

## VI. ASYMPTOTIC RESULTS FOR SMALL AND MODERATE FREQUENCIES: ANALYTIC EXPRESSION FOR DIELECTRIC RESPONSE

### A. SB model

Results can be obtained in analytical form by perturbation analysis of the SB model in the range of frequencies much smaller than $\omega_{2,3}$ where $\Sigma_2(\omega)\simeq\sigma_2$, $\Sigma_3(\omega)\simeq -i\omega C_3$, and $\omega C_3/\sigma_1\equiv 2\omega/\omega_{1,3}\ll 1$. Representing $\sigma$ as

$$\sigma\approx\sigma_1\left[f_0+2i\frac{\omega}{\omega_{1,3}}f_1\right] \tag{25}$$

and separating the terms of zero and first order in $\omega/\omega_{1,3}$, we obtain

$$f_0=\frac{-h_0+\sqrt{h_0^2-4b_0}}{2}\ , \tag{26}$$

$$f_1=\frac{\gamma/(1-d)^2-h_1f_0^2-b_1f_0}{3f_0^2+2f_0h_0+b_0}\ , \tag{27}$$

where

$$h_0=\frac{p_3+p_2-p_1(d-1)+\gamma[p_1+p_3-p_2(d-1)]}{d-1}\ , \tag{28}$$

$$h_1=\frac{p_1+p_2-(d-1)p_3}{d-1}\ , \tag{29}$$

$$b_0=\frac{\gamma[p_3-(p_1+p_2)(d-1)]}{(d-1)^2}\ , \tag{30}$$

$$b_1=\frac{p_2-(p_1+p_3)(d-1)+\gamma[p_1-(p_2+p_3)(d-1)]}{(d-1)^2}\ , \tag{31}$$

$$\gamma=\frac{\sigma_2}{\sigma_1}\ , \tag{32}$$

and

$$\mathrm{Re}\sigma=\sigma_1 f_0,\quad \chi'=C_3f_1\ . \tag{33}$$

Note that we defined all lengths in units of the lattice constant ($\approx$size of the particle); in order to restore the dimensional units one should replace $C_3$ by $C_3/l$. This refers to all the equations that contain $C_3$.

Similarly, one can obtain more general expressions for $\sigma'$ and $\chi'(\omega,x)$ in the region $\omega\lesssim\omega_{2,3}$. In this region

$$\begin{aligned}\mathrm{Re}\Sigma_3&=C_3\frac{\omega^2/\omega_{2,3}}{1+(\omega/\omega_{2,3})^2}\ ,\\ \mathrm{Im}\Sigma_3&=-\omega\frac{C_3}{1+(\omega/\omega_{2,3})^2}\end{aligned} \tag{34}$$

so that

$$\sigma'=\sigma_1\left[f_0+f_1\frac{4\omega^2}{\omega_{2,3}\omega_{1,3}}\frac{1}{1+(\omega/\omega_{2,3})^2}\right]\ , \tag{35}$$

$$\chi'(\omega,x)=\chi'(\omega=0)\frac{1}{1+(\omega/\omega_{2,3})^2}\ . \tag{36}$$

This supports our previous claim about the Lorentzian form of $\chi'(\omega,x)$.

For $d=3$ Eqs. (26)–(31) give expressions for $f_0$ and $f_1$ in a closed form as functions of $x$ and $\gamma$. They show, in particular, that $\chi'(0,x)$ has a maximum at the point $x_c$. We put down the expression for $f_1(x)$, obtained using the smallness of the parameter $\gamma$ close to the percolation threshold, $|x-0.577|>\gamma$,

$$\begin{aligned}f_1&\simeq f_{1R}\\ &=-9x^3(x-1)\frac{9x^4+(6-6\gamma)x^2+12\gamma x-6\gamma+1}{(3x^2-1)^3}\ ,\\ &\qquad x-0.577>\gamma\ ,\end{aligned} \tag{37}$$

$$\begin{aligned}f_1&\simeq f_{1L}=4.5\frac{x(x-1)^3}{(3x^2-1)(3x^2-3x+1)}+O(\gamma)\ ,\\ &\qquad x<0.577-\gamma\ .\end{aligned} \tag{38}$$

On the other hand at the point $x_c=0.577$

$$f_1 \approx 0.5\gamma^{u-1} = 0.5\gamma^{-0.5} . \quad (39)$$

Note that the effective-medium theory gives $u=0.5$, while the accepted value of the critical exponent in 3D is 0.72.[3] This could be used as a possible correction when applying the theory to experimental data.

For arbitrary $x$ one can use for estimates a formula which interpolates between (37), (38), and (39):

$$f_1 \approx 18x^3(1-x)^3\left\{36\gamma^{0.5}x^3(1-x)^3+(3x^2-1)\left[1-2x-x^2+6x^3-6x^4 +(1-2x+3x^2-6x^3-6x^4)\tanh\left[\frac{x-0.577}{\gamma}\right]\right]\right\}^{-1} \quad (40)$$

[see Fig. 10 for a comparison of (27) and (40)].

### B. LC model

One can obtain the expressions for $f_0$ and $f_1$ within the framework of the LC model by a replacement of $(d-1)$ by $q$ in Eqs. (26)–(31). In 3D ($q=3.7655$) the factor $f_1$ for small $\gamma$ in the region of parameters $|x-0.458|>\gamma$ takes the form

$$f_{1R} = 2.531\frac{x^3(1-x)}{(x^2-0.21)}, \quad x-0.458>\gamma , \quad (41)$$

$$f_{1L} = 0.266\frac{x(x-1)^3}{(x^2-x+0.395)(x^2-0.21)} , \quad x<0.458-\gamma . \quad (42)$$

At the maximum

$$f_1 \approx 0.266\gamma^{u-1} = 0.266\gamma^{-0.5} . \quad (43)$$

A unified interpolation formula can be built analogously to Eq. (40).

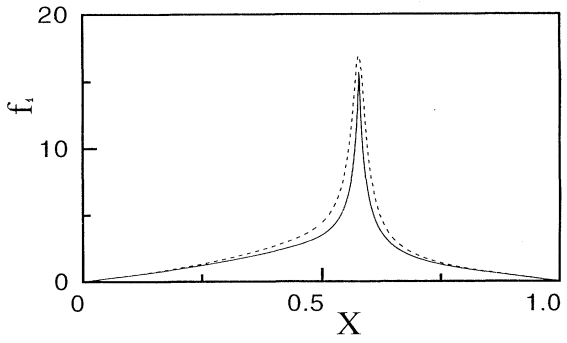


FIG. 10. A comparison of the interpolation formula (40) (solid line) and the result of the perturbation theory (27) (dashed line).

## VII. PERMITTIVITY MAXIMUM: ORDER OF MAGNITUDE ESTIMATE. THE DEPENDENCE ON TEMPERATURE AND OTHER FACTORS

The height of the maximum in the static dielectric susceptibility is evaluated (in dimensional units) as

$$\chi'_{\max} \approx \frac{C_3}{2l}\left[\frac{\sigma_1}{\sigma_2}\right]^{1-u} . \quad (44)$$

For typical values of the interfacial capacitance of the flat metal/solid-electrolyte interface per unit surface area $\sim 10\ \mu\mathrm{F/s\,m^2}$ and the size of the particles $\sim 1\ \mu\mathrm{m}^2$, $(C_3/l)\sim 10^3$. With the typical ratio $\sigma_1/\sigma_2 \sim 10^3$ and the effective-medium "modest" value of the exponent $u=0.5$ we get $\chi' \sim 10^4$, which gives an effective dielectric permittivity $\epsilon \sim 10^5$. This value can be increased to $10^7$ and greater values by the increase of the size of the grains (under an assumption that this procedure does not spoil the homogeneity of the sample, i.e., it does not induce porosity) which would enhance $C_3/l \sim l$ and using materials with greater ratio $\sigma_1/\sigma_2$. One may expect even greater enhancement if the contact between the metal and solid electrolyte grains had a fractal shape with the interface fractal dimension greater than 2.

How does the predicted effect depend on the variation of temperature, which does not destroy the composite? The height of the maximum in the static susceptibility $\chi'$ depends on it primarily due to $C_3$ and $\sigma_2$, since the temperature dependence of $\sigma$ is relatively weak. The temperature dependence of the characteristic frequency $\omega_{2,3}=2\sigma_2/C_3$ is determined by the same parameters. The temperature dependence of $C_3$ can be evaluated from the capacitance of the given metal/solid-electrolyte flat interface. Depending on the material it can vary several times usually increasing with temperature[23] (which may, simply, be a result of contact improvement). On the other hand, the conductivity of the solid electrolyte has an activational dependence $\sigma_2 \sim \exp\{-E/k_BT\}$ so that $\chi'_{\max} \sim C_3\exp\{(1-u)E/k_BT\}$ and $\omega_{2,3} \sim C_3^{-1}\exp\{-E/k_BT\}$. Which of the effects would

prevail? Solid conclusions can be made for a given combination of metal and solid electrolyte, having experimental data for the capacitance of the flat interface and the activation energy of ion diffusion; particularly strong effects could be expected near phase transitions if they confine the superionic state, which is not the case of zirconia electrolytes, however.

One effect can be predicted immediately. If the metal particles are covered by an oxide film, the maximum will decrease together with $C_3$. Indeed, in this case the capacitance of the oxide film is added in sequence to the double-layer capacitance; for a considerably thick film the former is smaller and will dominate in the overall capacitance.

## VIII. DISCUSSION

Earlier, Ukshe and Ukshe[27] have made an attempt to develop a Kirkpatrik-type effective medium theory for a two-bond model of a composite. The interface between the metal and solid electrolyte was taken into account in the equivalent scheme of the solid electrolyte particles, but the double-layer capacitance did not appear as a result of a contact between the metal and solid electrolyte grains. Presumably, this is the reason why the Ukshe and Ukshe model gave the two orders of magnitude enhancement of the sample geometrical capacitance near the percolation threshold instead of the four to six orders of magnitude typical for the three-bond model.

It is worthwhile to stress once more that the equations of the effective medium theory, homogeneous in space, cannot describe the case with the essentially inhomogeneous field distribution. Just such a situation takes place below the percolation threshold in the metallic component in the zero frequency limit: the static field, screened by the electrolyte, does not penetrate into the bulk of the composite. Thus, what Ukshe and Ukshe have calculated was the bulk impedance of the sample, which can be observed only at the sufficiently large frequencies (cf. Sec. I c). This makes the claims on the harmony of this model with the data of Bukun *et al.*[28] on the admittance of the carbon-$Ag_4$ $RbI_5$ unjustified. We believe that what Fig. 1 of Ref. 28 shows in the low-frequency limit is the *interfacial* capacitance, not described by the effective medium calculation. Indeed, the Lorentzian seen in Fig. 1 of Ref. 28 could not be the Lorentzian decay of the capacitance, predicted by the Ukshe and Ukshe model, because the experimental dispersion shown takes place at the frequencies at least three orders of magnitude lower than in the model. Also, the observed value of capacitance at $\omega \Longrightarrow 0$ is 200 times greater than the one predicted by the model. The quantity that the Ukshe and Ukshe model has actually attempted to calculate is the much smaller value of capacitance at $\omega > 10$ Hz. The same applies to the plot of the capacitance against the volume fraction of electrolyte shown for different frequencies (Fig. 3 of Ref. 28): while the curve 6 ($\omega = 20$ Hz) may have, in principle, a connection with the results of the effective medium theory, curve 1 cannot.

The data of Ref. 28 themselves are, nevertheless, very interesting. Figure 11 shows that they are in qualitative accordance with the equivalent circuit of Fig. 2 and Eqs. (5)–(8). Considering the case when the correlation length $\xi \propto l|x-x_c|^{-\nu} < L$ ($\nu = 0.9$ in 3D) we may suggest an extrapolation formula for the capacitance

$$C(x,\omega) = C_D/2 \frac{l^2}{L^2} \frac{|x-x_c|^{\mu} + (l/L)^3 f_0^2(x) f_1(x) (\omega/\bar{\omega})^2}{|x-x_c|^{2\mu} + (l/L)^4 f_0^2(x) (\omega/\bar{\omega})^2}. \tag{45}$$

Here $C_D$ is the capacitance of the interface between the

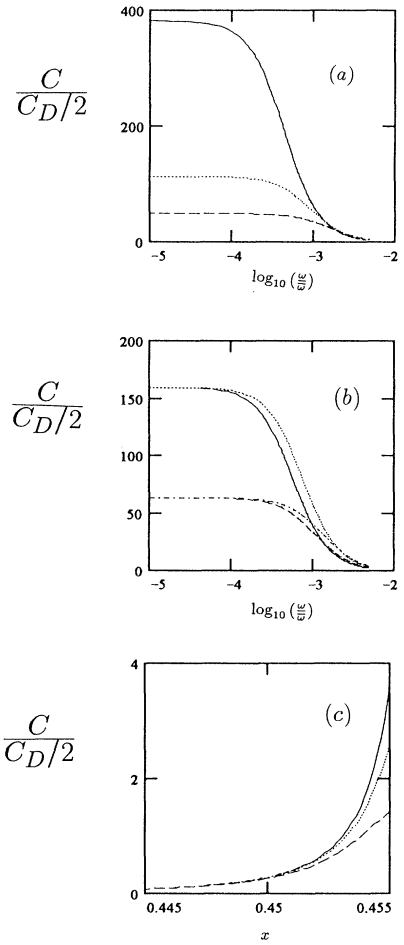


FIG. 11. The capacitance of the metal/composite/metal system near [below, $x_c - x > (L/l)^{1/\nu}, \gamma$] the percolation threshold, calculated via expression (45). Parameters $L/l = 10^3$, $\mu = 2.6$, $\gamma = 10^{-3}$, $x_c = 0.458$. (a) Frequency dependence of capacitance for different fractions of metallic component, $x$: —— 0.4575; · · · · 0.4572; — — — 0.4569. $\omega$ is given in units of $\bar{\omega}$, the frequency of charging of a flat metal/solid electrolyte/metal component. Calculated for the LC model. (b) Capacitance frequency dispersion: comparison of LC and SB models for the same "distance" $\Delta x = x_c - x$ from the percolation thresholds $x_c = 0.458$ and 0.577, respectively. Lower pairs of curves: $\Delta x = 0.007$ (—— SB; · · · · LC). Upper pair of curves: $\Delta x = 0.0001$ (— — —) SB; —·—·— LC). (c) The capacitance as a function of the volume fraction of the metallic component for different frequencies. SB model. $\omega$: (——) 0; (· · · ·) $0.005\bar{\omega}$; (— — —) $0.01\bar{\omega}$.

ideal flat metal and the homogeneous electrolyte, $\bar{\omega}$ is the frequency of charging the double layer at a flat surface via the migration of ions through the bulk of the solid electrolyte: $\bar{\omega}=2/[C_D R_g(x=0)]$, $f_0(x)$ and $f_1(x)$ are given by the corresponding equations of the SB and LC models, respectively, and $\mu=D_i\nu$, where $D_i$ is the Hausdorf dimension of the surface of percolation clusters. Note that in deriving (45) we have neglected the possible fractal structure of the grain surfaces. Figure 11(a) displays the family of $C(\omega)$ curves for different $x$ values, for the LC model. $f_1(x)$ are given by Eq. (42), $x_c=0.458$. In Fig. 11(b), the LC model is compared with the SB model. A difference between the curves is seen together with the onset of frequency dispersion. The difference at intermediate frequencies is due to the variation in conductivities given by these two models. In the high-frequency limit (not shown) the difference is due to different values of the geometrical capacitance.

Figure 11(c) displays $C(x)$ for different frequencies below the percolation threshold in the volume portion of the metal. The capacitance at zero frequency is entirely determined by the capacitance of the interface.

We have deliberately plotted curves very close to the percolation threshold, where the difference between the bulk and surface contribution is most clearly seen, but assuming warranted that the size of the system is much greater than $l/(\Delta x)^{\nu}$. The crude picture of the interplay between the bulk and surface contributions sketched in the Introduction and discussed in this section should in no way be regarded as a *solution* of the problem. Future theory or computer siulation for a finite-size system with proper boundary conditions would tell us what is the true response function of the whole system at the intermediate frequencies and how the crossover between the bulk and surface responses takes place. For relatively thin samples, when the correlation length (which grows with the approach to the percolation threshold) becomes comparable with the thickness of the sample, there will be no separate bulk and surface contributions, and the interpolations like the one discussed above will be at least inaccurate, if not misleading.

## IX. CONCLUSION AND OUTLOOK

We have considered a metal–solid-electrolyte ceramic mixture as a random network of three types of bonds, representing, respectively, the conductances of metallic and solid electrolyte particles and the admittance of the contact between them.

This metal–solid-electrolyte contact is blocking in the absence of Faraday processes, and the third bond contributes to the system equivalent circuit the double-layer capacitance of the metal–solid-electrolyte interface, a quantity orders of magnitude larger than the geometrical capacitance of a solid electrolyte grain. Close to the percolation threshold for electronic conductivity this gives rise to a strong enhancement of the imaginary part of the system conductivity, i.e., to a peak in dielectric permittivity which, as we show, can easily reach the value of $10^5$. Even greater values (up to $10^7$) can be obtained in principle for particularly large ratios of the conductivity of the metal to the conductivity of the solid electrolyte and large double-layer capacitances which could be provided by the proper choice of the components of the ceramic material and large surface area of the interface between two metal and solid electrolyte grains.

The enhancement decreases with increasing frequency. Indeed, when it becomes larger than the inverse time of ion migration through the solid electrolyte grains, the countercharge at each blocking metal/electrolyte grain contact has "no time" to react to the variation of the charge on the metal and the contribution of the imaginary resistors vanishes. This leads to a Lorentzian shape of the dielectric permittivity frequency dependence.

Within the scope for the three-bond random network we obtained the effective-medium solutions, which are normally inaccurate at the percolation thresholds, but usually work satisfactorily outside the critical region. Thus the results await a comparison with computer simulation and real-space renormalization methods. We expect, however, the prediction of the *peak in the dielectric permittivity close to the percolation threshold* to survive. It is, of course, an open question how broad the frequency window would be where this "bulk" effect could be observed at the background of the surface contribution. The above given estimates suggest that the effect ought to be looked for in the range 1–100 Hz, but this is only a guess. Since the theory for heterogeneous systems—with the boundary conditions in confined geometry—is not yet developed, we can only speculate on the interplay of the surface and bulk contributions, but cannot make any solid conclusions *a priori*. The latter is particularly dangerous for a sample the thickness of which is only a few times larger than the percolation correlation length, where there is no "bulk" as such.

Experimental observation of this effect may be affected by random fluctuations of bond admittances along the sample. For instance, they may be caused by variation of the contact area between the grains (admittance of the third bond is proportional to the contact area), even if they are morphologically of the same size: some grains are pressed to each other more tightly than others. Random fluctuations of the grain size may also contribute significantly to the system macroscopic properties. Variations of the grain shape or of the phase state (grains could be "liquidlike") may be of a certain importance. The presence of pores can modify the results. Because of these factors an experimental observation of the predicted enhancement of the dielectric permittivity is to be started with a specially designed monodisperse ceramic mixture with a small percentage of pore space and monodipersive pore-radii distribution, compatible with the model system considered above.

The predicted giant enhancement of the bulk dielectric permittivity of the composite, if confirmed by experiments, however, cannot be utilized for energy storage in supercapacitors based on MCM structures. Static accumulation of energy depends completely on the interfacial capacitance. However, the resonance in $\epsilon$ will give rise to an enhancement of the geometrical capacitance of the sample, which could be of some interest for the frequency characteristics of supercapacitors.

## ACKNOWLEDGMENTS

The authors are grateful to J. Divisek, B. de Haart, H. Hermann, P. Duxbury, D. Stauffer, A. M. Kuznetzov, M. Leibig, B. Noethe, I. C. Vinke, and U. Stimming for useful discussions and consultations. Special thanks are due to A. S. Ioselevich for a critical reading of the manuscript and important criticisms and suggestions. The support given to S.G. by the MINERVA foundation and to A.N. by CNRS (France) is gratefully acknowledged.

---

*The address for correspondence.

[1]C. S. Chen, B. A. Boukamp, H. J. M. Bouwmeester, G. Z. Cao, H. Krudoff, A. J. Winnubst, and A. J. Burgraaf, Solid State Ionics **76**, 23 (1995).

[2]F. H. van Heuveln, F. P. F. van Berkel, and I. P. P. Huijsmans, in *High Temperature Electrochemical Behavior of Fast Ion and Mixed Conductors,* Proceedings of the 14th Risø International Symposium on Material Science, edited by F. W. Poulsen, J. J. Bentzen, T. Jacobsen, E. Skou, and M. J. L. Østergård (RISØ, Roskilde, 1993), p. 53.

[3]J. P. Clerc, G. Giraud, J. M. Laugier, and J. M. Luck, Adv. Phys. **39**, 191 (1990).

[4]D. J. Bergman and D. Stroud, in *Solid State Physics: Advances in Research and Applications,* edited by H. Ehrenreich and D. Turnbull (Academic, Boston, 1992), Vol. 46, p. 147.

[5]D. Stauffer and A. Aharony, *Introduction to Percolation Theory* (Taylor & Francis, London, 1992).

[6]S. Kirkpatrick, Rev. Mod. Phys. **45**, 574 (1973).

[7]B. P. Watson and P. L. Leath, Phys. Rev. B **11**, 4893 (1974).

[8]L. Webman, J. Jortner, and M. H. Cohen, Phys. Rev. B **11**, 2885 (1975).

[9]J. P. Straley, J. Phys. C **9**, 783 (1976).

[10]A. L. Efros and B. I. Shklovski, Phys. Status Solidi B **76**, 475 (1976).

[11]J. Bernasconi and H. J. Wiesmann, Phys. Rev. B **13**, 1131 (1976).

[12]D. Stroud and D. J. Bergman, Phys. Rev. **25**, 2061 (1982).

[13]A. P. Vinogradov, A. M. Karimov, A. I. Kunavin, A. N. Lagar'kov, A. K. Sarychev, and N. A. Stember, Sov. Phys. Dokl. **29**, 214 (1984).

[14]R. S. Koss and D. Stroud, Phys. Rev. B **35**, 9004 (1987).

[15]R. Blender and W. Dietrich, J. Phys. C **20**, 6113 (1987).

[16]A. Coniglio, M. Daoud, and H. J. Herrmann, J. Phys. A **22**, 4189 (1989).

[17]A. A. Kornyshev and M. A. Vorotyntsev, Electrochim. Acta **26**, 303 (1981).

[18]B. B. Owens, J. E. Oxley, and A. F. Sammels, in *Solid Electrolytes,* edited by S. Geller (Springer, Berlin, 1977).

[19]A. Le Mehaute and G. Crepy, Solid State Ionics **9**, 17 (1983).

[20]For a review see S. H. Liu, in *Condensed Matter Physics Aspects of Electrochemistry,* edited by M. P. Tosi and A. A. Kornyshev (World Scientific, Singapore, 1991), p. 329.

[21]R. De Levie, Electrochim. Acta **10**, 113 (1965).

[22]T. C. Halsey and M. Leibig, Ann. Phys. (N.Y.) **219**, 109 (1992).

[23]T. C. Halsey, Phys. Rev. A **38**, 4789 (1989).

[24]E. A. Ukshe and N. G. Bukun, *Solid Electrolytes* (Nauka, Moscow, 1977); in *Impedance Spectroscopy,* edited by J. Ross Macdonald (John Wiley & Sons, New York, 1987).

[25]It is important to note that this formal limit is not a limiting case of the metal/dielectric mixture. Indeed, the system in which the dielectric particles contribute to the equivalent circuit of the third bond a capacitance equal to the capacitance of the grains of the solid electrolyte is obtained by a formal limiting case (Ref. 26) of our theory ($C_3=\infty$, $\sigma_2=0$). Here we do not obtain the two-bond limit since the metal/dielectric interface has an equivalent circuit with conductance ($\approx\sigma_1$) in sequence with the small capacitance ($\approx C_2$). In most of the theories of metal/dielectric mixtures this third bond is ignored. We made a comparison between the limiting case of the metal/dielectric mixture in our three-bond model and the results of the two-bond model. They are qualitatively the same at small $\omega$.

[26]This is, really, only a formal mathematical limit, since this equivalent circuit is approximate and valid when $C_3 \gg C_2$. Putting the number of charge carriers in the ionic conductor to zero, which does give the limit of an insulator, cannot be considered physically within this equivalent circuit.

[27]A. E. Ukshe and E. A. Ukshe, Elektrokhimiya **17**, 649 (1981) [Sov. Electrochem. **17**, 531 (1981)].

[28]N. G. Bukun, A. E. Ukshe, A. M. Vakulenko, and L. O. Atovmyan, Elektrokimiya **17**, 606 (1981) [Sov. Electrochem. **17**, 496 (1981)].